ACS OMEGA

Open Access

This article is licensed under CC-BY-NC-ND 4.0

http://pubs.acs.org/journal/acsodf

Article

Halogen Bonding in the Decoration of Secondary Coordination Sphere of Zinc(II) and Cadmium(II) Complexes: Catalytic Application in Cycloaddition Reaction of CO_2 with Epoxides

Vusala A. Aliyeva, Ana B. Paninho, Ana V. M. Nunes,* Anirban Karmakar, Atash V. Gurbanov, Arianna R. Rutigliano, Emma Gallo, Kamran T. Mahmudov,* and Armando J. L. Pombeiro*

Cite This: *ACS Omega* 2023, 8, 42290−42300

Read Online

ACCESS | Metrics & More | Article Recommendations | Supporting Information

ABSTRACT: Three new zinc(II) complexes $[Zn(H_2L^3)_2(H_2O)_3]$ (**Zn2**), $[Zn(H_3L^{2a})(H_2O)_3]_n$ (**Zn3**) (H_3L^{2a} = 2,4-diiodo-5-(2-(2,4,6-trioxotetrahydropyrimidin-5(2*H*)-ylidene)hydrazineyl)isophthalate) and $[Zn(HL^4)(DMF)(H_2O)]_n$ (**Zn4**) were synthesized by the reaction of Zn(II) salts with 5-(2-(2,4-dioxopentan-3-ylidene)-hydrazineyl) isophthalic acid (H_3L^3), 2,4,6-triiodo-5-(2-(2,4,6-trioxotetrahydropyrimidin-5(2*H*)-ylidene)hydrazineyl) isophthalic acid (H_5L^2) (in the presence of $NH_2OH{\cdot}HCl$) and 5-(2-(2,4-dioxopentan-3-ylidene)hydrazineyl)-2,4,6-triiodoisophthalic acid (H_3L^4), respectively. According to the X-ray structural analysis, the intramolecular resonance-assisted hydrogen bond ring remains intact, with N···O distances of 2.562(5) and 2.573(5) Å in **Zn2**, 2.603(6) Å in **Zn3**, and 2.563(8) Å in **Zn4**. In the crystal packing of **Zn3**, the cooperation of I···O and I···I types of halogen bonds between tectons leads to a one-dimensional supramolecular polymer, while I···O interactions aggregate 1D chains of coordination polymer **Zn4**. These new complexes (**Zn2**, **Zn3**, and **Zn4**) and known $[Zn(H_3L^1)(H_2O)_2]_n$ (**Zn1**) (H_3L^1 = 5-(2-(2,4,6-trioxotetrahydropyrimidin-5(2*H*)-ylidene) hydrazineyl)isophthalate), $\{[Zn(H_3L^1)(H_2O)_3]{\cdot}3H_2O\}_n$ (**Zn5**), $[Cd(H_3L^1)(H_2O)_2]_n$ (**Cd1**), $\{[Cd(HL^3)(H_2O)_2(DMF)]{\cdot}H_2O\}_n$ (**Cd2**), $[Cd(H_3L^3)]_n$ (**Cd-3**), $\{[Cd_2(\mu\text{-}H_2O)_2(\mu\text{-}H_2L^4)_2(H_2L^4)_2]{\cdot}2H_2O\}_n$ (**Cd4**), and $\{[Cd(H_3L^1)(H_2O)_3]{\cdot}4H_2O\}_n$ (**Cd5**) were tested as catalysts in the cycloaddition reaction of CO_2 with epoxides in the presence of tetrabutylammonium halides as the cocatalyst. The halogen-bonded catalyst **Zn4** is the most efficient one in the presence of tetrabutylammonium bromide by affording a high yield (85−99%) of cyclic carbonates under solvent-free conditions after 48 h at 40 bar and 80 °C.

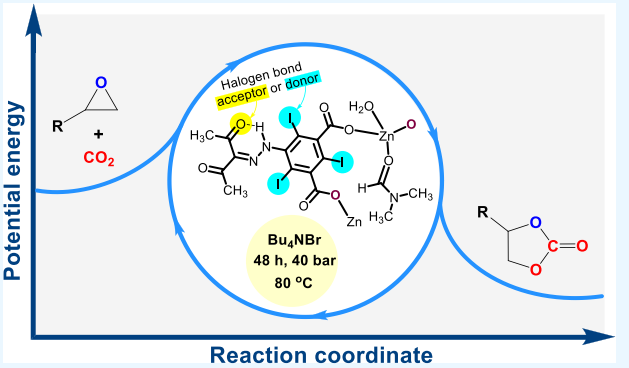

1. INTRODUCTION

Due to the progress of human civilization and development of the chemical industry, the atmospheric CO_2 concentration has increased from ca. 280 ppm (in the early 1800s) to 417 ppm (in 2022), and the Intergovernmental Panel on Climate Change is predicting it to reach 950 ppm by 2100.[1−3] As a result, the excessive accumulation of a predominant greenhouse gas (CO_2) on Earth's ecosystems is a major cause of glacier melting, global warming, and other climate change issues.[4] In order to reduce or remain fairly stable the CO_2 emissions, we must keep under control/monitor the industrial processes and develop new energy efficient technologies. Among the strategies for decreasing emissions and mitigating atmospheric CO_2, (i) CO_2 capture and storage and (ii) CO_2 capture and utilization are expected to play important roles.[5] Development of an effective CO_2 conversion into high value-added chemicals and fuels has emerged as one of the active research topics in recent years.[6−11] In industry, CO_2 is mainly used as a chemical feedstock in the synthesis of urea, methanol, salicylic acid, and organic carbonates.[12]

Due to the high bonding enthalpy of the C═O double bond (+805 kJ mol^{-1})[13] and the linear molecular configuration of centrosymmetric CO_2, a catalyst is generally required to bring down the energy barrier in its chemical transformations. The organocatalytic and metal complex catalyzed conversion of CO_2, as an abundant, inexpensive, nontoxic, nonflammable, and renewable C1 source/building unit (instead of the commonly used phosgene, $COCl_2$) in chemical synthesis has already been recognized as a powerful synthetic strategy.[1−25]

Received: June 19, 2023
Accepted: September 28, 2023
Published: November 1, 2023

Downloaded via UNIV NOVA DE LISBOA 00900 on March 4, 2024 at 16:03:39 (UTC).
See https://pubs.acs.org/sharingguidelines for options on how to legitimately share published articles.

© 2023 The Authors. Published by American Chemical Society

Scheme 1. Arylhydrazones of Isophthalic Acid (AHIPA) and Their Iodine-Substituted Analogs

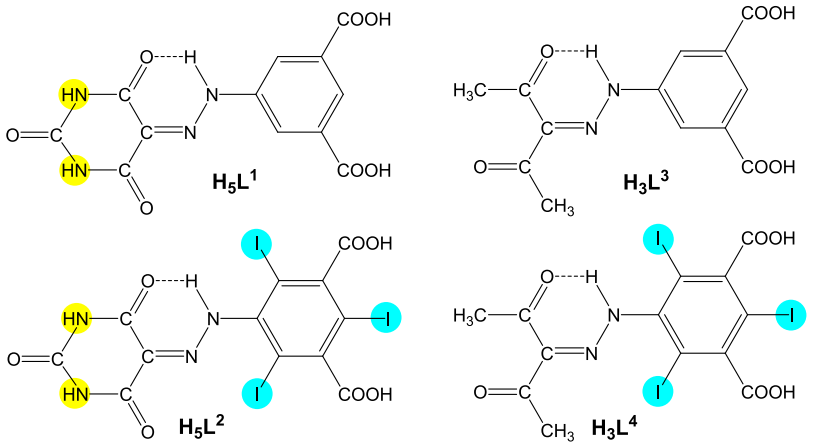

Scheme 2. Zn(II) and Cd(II) Complexes of Arylhydrazone Ligands; the New Compounds Zn2−Zn4 Are Highlighted in Green Color

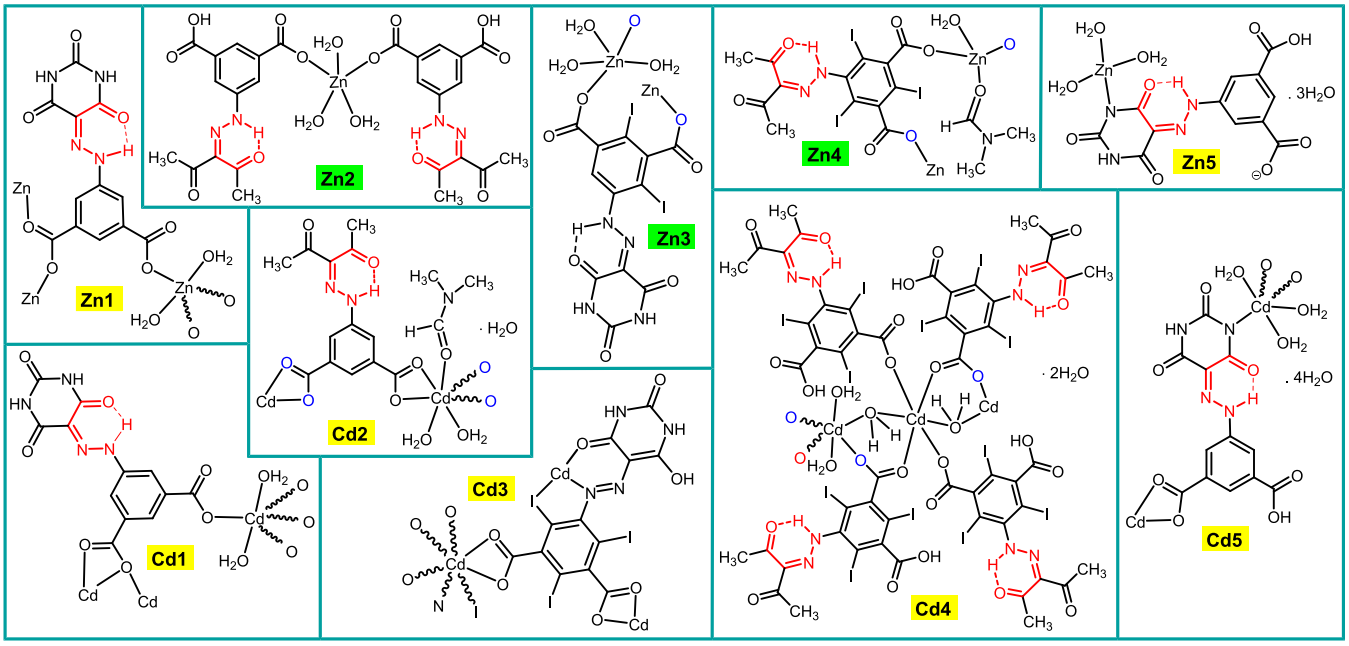

For example, metal complex-catalyzed cycloaddition of CO_2 with epoxides leads to cyclic and/or polymeric carbonates,[14−25] which find a variety of applications in the pharmaceutical industry,[26−28] electrolytes in lithium ion batteries,[29,30] paint-strippers,[31] aprotic polar solvents in organic synthesis,[32,33] intermediates in the synthesis of carbamates,[34,35] etc. The search for a new effective, environmentally friendly, and inexpensive catalytic system is a tremendous challenge in the synthesis of cyclic carbonates from the CO_2 and epoxides.

On the other hand, decoration of the secondary coordination sphere of metal complexes is a recognized synthetic strategy in catalysis.[36,37] Similarly to hydrogen bonds, other weak interactions such as halogen,[38] chalcogen,[39] and pnictogen[40] bonds can also be used in the crystal engineering of metal complexes and enhance their functional properties.[41] For example, due to the high directionality, these weak forces have been employed as selectivity directing tools in homogeneous catalysis.[42] The application of halogen bonded metal complexes as catalysts in the reaction of CO_2 with epoxides had not yet been reported, whereas there are only two examples of the halogen bond involved organocatalytic version of this reaction.[43,44]

Considering all the above points, in this work, we focused on the following aims: (i) to design the secondary coordination sphere of new Zn(II)-arylhydrazone complexes with hydrogen bond and halogen bond donor centers (Schemes 1 and 2); (ii) to study the influence of methylene active fragments (comparing acetylacetone with barbituric acid, see Scheme 1), halogens (comparing isophthalic and 2,4,6-triiodoisophthalic fragments in arylhydrazone ligands, see Scheme 1) and metal centers (comparing Zn with Cd, see Scheme 2) on Zn(II)- or Cd(II)-catalyzed cycloaddition of CO_2 with epoxides.

2. EXPERIMENTAL SECTION

2.1. Materials and Instrumentation. All chemicals were obtained from commercial sources and used as received. The synthesis and characterization of 5-(2-(2,4,6-trioxotetrahydro-

https://doi.org/10.1021/acsomega.3c04262
ACS Omega 2023, 8, 42290−42300

Table 1. Crystallographic Data and Structure Refinement Details for Zn2, Zn3, and Zn4

Identification name	Zn2	Zn3	Zn4
Formulas	$C_{26}H_{28}N_4O_{15}Zn$	$C_{12}H_{10}I_2N_4O_{10}Zn$	$C_{16}H_{16}I_3N_3O_8Zn$
Mol. wt.	701.89	689.41	824.39
Crystal system	Triclinic	Triclinic	Monoclinic
Space group	*P-1*	*P-1*	*P21c*
Temperature/K	296	296	296
Wavelength /Å	0.71073	0.71073	0.71073
a /Å	7.4901(16)	7.4035(6)	17.972(3)
b /Å	8.8763(18)	9.4276(9)	7.7821(12)
c /Å	24.455(5)	14.1061(16)	17.281(3)
α/°	88.773(8)	103.836(4)	90
β/°	87.729(8)	100.670(3)	105.292(5)
γ/°	65.960(8)	101.367(4)	90
V/ Å^3	1483.7(5)	908.92(16)	2331.3(6)
Z	2	2	4
Density/Mgm^{-3}	1.571	2.519	2.349
Abs. Coeff. /mm^{-1}	0.909	4.812	5.072
F(000)	724	652	1544
Refl. Collected	15830	19213	30494
Refl. Unique	4682	3733	3970
Max. 2θ/°	25.431	26.444	24.717
Complete to 2θ (%)	95.5	99.4	99.9
Refl. with I > 2σ(I)	6642	3233	3294
Data/Restraints/Parameters	4682/0/420	3733/4/282	3970/0/312
Goof (F^2)	1.087	1.062	1.102
R1 [I > 2s(I)][a]	0.0593	0.0411	0.0380
wR2 [I > 2s(I)][b]	0.1882	0.1085	0.0697
R1 [all data]	0.0698	0.0484	0.0510
wR2 [all data]	0.2059	0.1140	0.0739

[a] $R1 = \Sigma||F_0| - |F_c||/\Sigma|F_0|$. [b] $wR2 = [\Sigma[w(F_0^2 - F_c^2)^2]/\Sigma[w(F_0^2)^2]]^{1/2}$.

pyrimidin-5(2*H*)-ylidene)hydrazineyl)isophthalic acid (H_5L^1), 2,4,6-triiodo-5-(2-(2,4,6-trioxotetrahydropyrimidin-5(2*H*)-ylidene)hydrazineyl) isophthalic acid (H_5L^2), 5-(2-(2,4-dioxopentan-3-ylidene)hydrazineyl)isophthalic acid (H_3L^3), and 5-(2-(2,4-dioxopentan-3-ylidene)hydrazineyl)-2,4,6-triiodoisophthalic acid (H_3L^4) were reported earlier.[41,45,46] The complexes $[Zn(H_3L^1)(H_2O)_2]_n$ (**Zn1**), $\{[Zn(H_3L^1)(H_2O)_3]\cdot 3H_2O\}_n$ (**Zn5**), $[Cd(H_3L^1)(H_2O)_2]_n$ (**Cd1**), $\{[Cd(HL^3)(H_2O)_2(DMF)]\cdot H_2O\}_n$ (**Cd2**), $[Cd(H_3L^3)]_n$ (**Cd3**), $\{[Cd_2(\mu\text{-}H_2O)_2(\mu\text{-}H_2L^4)_2(H_2L^4)_2]\cdot 2H_2O\}_n$ (**Cd4**), and $\{[Cd(H_3L^1)(H_2O)_3]\cdot 4H_2O\}_n$ (**Cd5**) were previously reported by us.[41,45] The IR spectra (4000−400 cm^{-1}) were recorded on a Bruker Alpha-P ATR-IR spectrometer. The ^{1}H and ^{13}C NMR spectra were obtained at room temperature (r.t.) on a Bruker 400.13 MHz spectrometer using tetramethylsilane [$Si(CH_3)_4$] as the internal reference. Carbon, hydrogen, and nitrogen elemental analyses were carried out by the Microanalytical Service of the Instituto Superior Técnico. Electrospray mass spectrometry (ESI-MS) was run with an ion-trap instrument (Varian 500-MS LC Ion Trap Mass Spectrometer) equipped with an electrospray ion source. For electrospray ionization, the drying gas and flow rate were optimized according to the particular sample with 35 psi nebulizer pressure. Scanning was performed from *m*/*z* 0 to 1500 in methanol solution. The compounds were observed in the positive or negative ion mode (capillary voltage = 80−105 V).

2.2. Synthesis of Zn(II)-Arylhydrazone Complexes. *[Zn(H$_2$L^3)$_2$(H$_2$O)$_3$] (**Zn2**).* A mixture of H_3L^3 (15 mg, 0.05 mmol) and $Zn(NO_3)_2\cdot 6H_2O$ (15 mg, 0.05 mmol) was dissolved in 3 mL of ethanol. The resulting mixture was sealed in an 8 mL glass vessel and heated to 65 °C for 48 h. Subsequent gradual cooling to room temperature (0.2 °C min^{-1}) afforded colorless crystals of **Zn2**. Yield: 65% (based on Zn). Anal. calcd for $C_{26}H_{28}N_4O_{15}Zn$ (M = 701.90): C, 44.49; H, 4.02; N, 7.98; found: C, 44.46; H, 4.00; N, 7.95. IR (ATR, 298 K): 1625 ν(C═O) and 1513 ν(C═N) cm^{-1}. MS (ESI, positive ion mode), *m*/*z*: 648.86 [*Mr*−3H$_2$O+H$^+$].

*[Zn(H$_3$L^{2a})(H$_2$O)$_3$]$_n$ (**Zn3**).* A mixture of H_5L^2 (35 mg, 0.05 mmol), $Zn(CH_3COO)_2\cdot 2H_2O$ (11 mg, 0.05 mmol) and $NH_2OH\cdot HCl$ (4 mg, 0.057 mmol) was dissolved in 10 mL of methanol. The resulting mixture was left at room temperature for slow evaporation; colorless crystals of **Zn3** suitable for X-rays started to form after *ca.* 2 days. Yield: 69% (based on Zn). Anal. calcd for $C_{12}H_{10}I_2N_4O_{10}Zn$ (M = 689.42): C, 20.91; H, 1.46; N, 8.13; found: C, 20.88; H, 1.45; N, 8.09. IR (ATR, 298 K): 1699 ν(C═O) and 1595 ν(C═N) cm^{-1}. MS (ESI, positive ion mode), *m*/*z*: 636.37 [*Mr*−3H$_2$O +H$^+$].

*[Zn(HL^4)(DMF)(H$_2$O)]$_n$ (**Zn4**).* A mixture of H_3L^4 (34 mg, 0.05 mmol) and $Zn(CH_3COO)_2\cdot 2H_2O$ (11 mg, 0.05 mmol) was dissolved in 3 mL of ethanol/DMF (30/1, v/v). The resulting mixture was left at room temperature for slow evaporation; colorless crystals of **Zn4** suitable for X-rays started to form after *ca.* 5 days. Yield: 54% (based on Zn). Anal. calcd for $C_{16}H_{16}I_3N_3O_8Zn$ (M = 824.41): C, 23.31; H, 1.96; N, 5.10; found: C, 23.28; H, 1.95; N, 5.07. IR (ATR, 298 K): 1595 ν(C═O) and 1498 ν(C═N) cm^{-1}. MS (ESI, positive ion mode), *m*/*z*: 734.30 [*Mr*−DMF−H$_2$O+H$^+$].

2.3. X-ray Analysis. X-ray diffraction patterns of **Zn2**, **Zn3**, and **Zn4** were collected using a Bruker SMART APEX-II CCD

https://doi.org/10.1021/acsomega.3c04262
ACS Omega 2023, 8, 42290−42300

area detector equipped with graphite-monochromated Mo−Kα radiation (λ = 0.71073 Å) at 296(2) K (Table 1). Absorption correction was applied by SADABS.[47,48] The structures were solved by direct methods and refined on F^2 by full-matrix least-squares using Bruker's SHELXTL-97.[49] All nonhydrogen atoms were refined anisotropically. The hydrogen atoms were inserted at the calculated positions. Crystallographic data for the structural analysis have been deposited to the Cambridge Crystallographic Data Center (CCDC 2248269 for **Zn2**, 2248270 for **Zn3**, and 2248271 for **Zn4**). A copy of this information can be obtained free of charge from The Director, CCDC, 12 Union Road, Cambridge CB2 1EZ, UK (Fax: (+44) 1223−336033; E-mail: deposit@ccdc.cam.ac.uk or www.ccdc.cam.ac.uk/data_request/cif).

2.4. Catalytic Activity Studies. The coupling reaction of CO_2 with epoxide was performed following an experimental procedure earlier described.[24] All reactions were performed in stainless steel (11 mL) high-pressure reactors equipped with two sapphire windows, which allowed a direct visualization of the internal volume (Figure 1). A typical experiment consisted

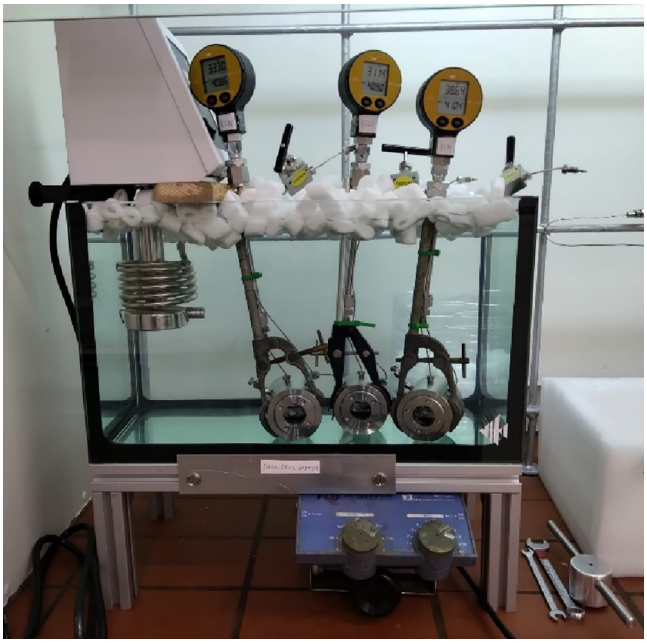

Figure 1. High pressure reactors in a water bath.

of loading the reactor with the catalyst, cocatalyst, and epoxide. A magnetic stirring bar was used to ensure an efficient mixing of the reaction mixture. After the reactor is closed, a small amount of CO_2 is introduced into the system through an inlet high-pressure valve. The pressure within the system was measured by a Setra pressure transducer (model 204) with accuracy of determination ±0.007 MPa. The reactor is then immersed in a water bath previously heated to the desired temperature using a temperature controller (Selecta Thermotronic II) with a precision of ±0.1 °C. Finally, the CO_2 pressure is increased until the desired value is reached. After the completion of the reaction, the reactor was cooled, and excess CO_2 was released slowly before a known amount of mesitylene and 0.3 mL of $CHCl_3$ were added and mixed. Next, an aliquot of the resulting mixture was taken and analyzed by NMR spectroscopy (Bruker Avance III 400 MHz) with $CDCl_3$ as a solvent. Thus, the NMR yield is calculated from the integration of the peaks characteristic of the mesitylene, epoxy and carbonate C_β−H (methine) at the ^{1}H NMR spectrum of this crude sample and comparison to published spectra.[50−56] It should be noted that the selectivity toward cyclic carbonate formation was >99%, and no other byproducts were detected.

3. RESULTS AND DISCUSSION

3.1. Synthesis and Characterization of Zn(II)-Arylhydrazones. The solvothermal reaction of $Zn(NO_3)_2{\cdot}6H_2O$ with 5-(2-(2,4-dioxopentan-3-ylidene)hydrazineyl)iso-phthalic acid (H_3L^3) in ethanol at 65 °C for 48 h leads to the monomeric Zn(II) complex, $[Zn(H_2L^3)_2(H_2O)_3]$ (**Zn2**) (Scheme 2). Meanwhile, the reaction of $Zn(CH_3COO)_2{\cdot}2H_2O$ with 2,4,6-triiodo-5-(2-(2,4,6-trioxotetrahydropyrimidin-5(2*H*)-ylidene)hydrazineyl)isophthalic acid (H_5L^2) or 5-(2-(2,4-dioxopentan-3-ylidene)hydrazineyl)-2,4,6-triiodoisophthalic acid (H_3L^4) in the presence or absence of $NH_2OH{\cdot}HCl$ in methanol or ethanol/DMF (30/1, v/v) at room temperature affords the coordination polymer $[Zn(H_3L^{2a})(H_2O)_3]_n$ (**Zn3**) or $[Zn(HL^4)(DMF)(H_2O)]_n$ (**Zn4**), respectively (Scheme 2). It should be noted that in complexation in the presence of $NH_2OH{\cdot}HCl$ (to form **Zn3**) one C−I bond cleavage occurs at the aromatic moiety of H_5L^2 leading to 2,4-diiodo-5-(2-(2,4,6-trioxotetrahydropyrimidin-5(2*H*)-ylidene) hydrazineyl)-isophthalate $(H_3L^{2a})^{2-}$ (Scheme 2). All three compounds were characterized by IR spectroscopy, ESI-MS spectra, elemental analysis, and single crystal X-ray diffraction. In the IR spectra of **Zn2**, **Zn3**, and **Zn4**, the ν(C═O) and ν(C═N) signals appear at 1625 and 1513, 1699 and 1595, and 1595 and 1498 cm^{-1}, respectively, which are values that are significantly shifted in relation to the corresponding signals of (1654 and 1558) H_3L^3, (1670 and 1494) H_5L^2, and (1614 and 1491) H_3L^4 ligands.[41] The major fragmentation peaks in the ESI-MS spectra of the compounds in methanol solution can be assigned as follows: 648.86 $[Zn(H_2L^3)_2{+}H^+]$ for **Zn2**, 636.37 $[Zn(H_3L^{2a}){+}H^+]$ for **Zn3**, and 734.30 $[Zn(HL^4){+}H^+)]$ for **Zn4**. Both elemental analyses and X-ray crystallography (see below) are consistent with the proposed formulations.

The bis-ligand mononuclear complex **Zn2** crystallizes in the triclinic crystal system and space group *P*1 (Table 1, Figure 2). Each coordinating arylhydrazone exists as a monoanion acting as a monodentate ligand. In the complex, the zinc atom is five-coordinated in a distorted trigonal-bipyramidal ZnO5 environment, in which the basal coordination sites are occupied by three oxygen atoms (O1, O7, and O14), with bond lengths of 1.952(3), 1.967(4), and 2.008(4) Å, respectively. The axial positions are occupied by two oxygen atoms (O13 and O15) from water molecules, with bond lengths of 2.165(4) and 2.138(4) Å, respectively. In both coordinated ligands in **Zn2** the resonance assisted hydrogen bond (RAHB) system N1−H1···O6 and N3−H3···O11 remains intact, with N···O distances of 2.562(5) and 2.573(5) Å, respectively (Figure 2), which falls in the average N···O distance range (2.538−2.661 Å) observed for other arylhydrazones of active methylene compounds.[57−59] In the crystal packing of **Zn2**, the molecules are linked by O(4)−H(4)···O(2) (2.630 Å) and O(9)−H(9)···O(8) (2.720 Å) hydrogen bonds, which generate $R_2^2(24)$ ring motifs,[60] resulting in a 1D supramolecular chain (Figure S1).

The five-coordinate Zn(II) center in **Zn3** adopts a distorted trigonal-bipyramidal geometry (τ_5 = 0.75),[61] ligated by two arylhydrazone ligands and three water molecules (Figure 2). The zinc atom sits almost in the trigonal plane of the O1O4O8

https://doi.org/10.1021/acsomega.3c04262
ACS Omega 2023, 8, 42290−42300

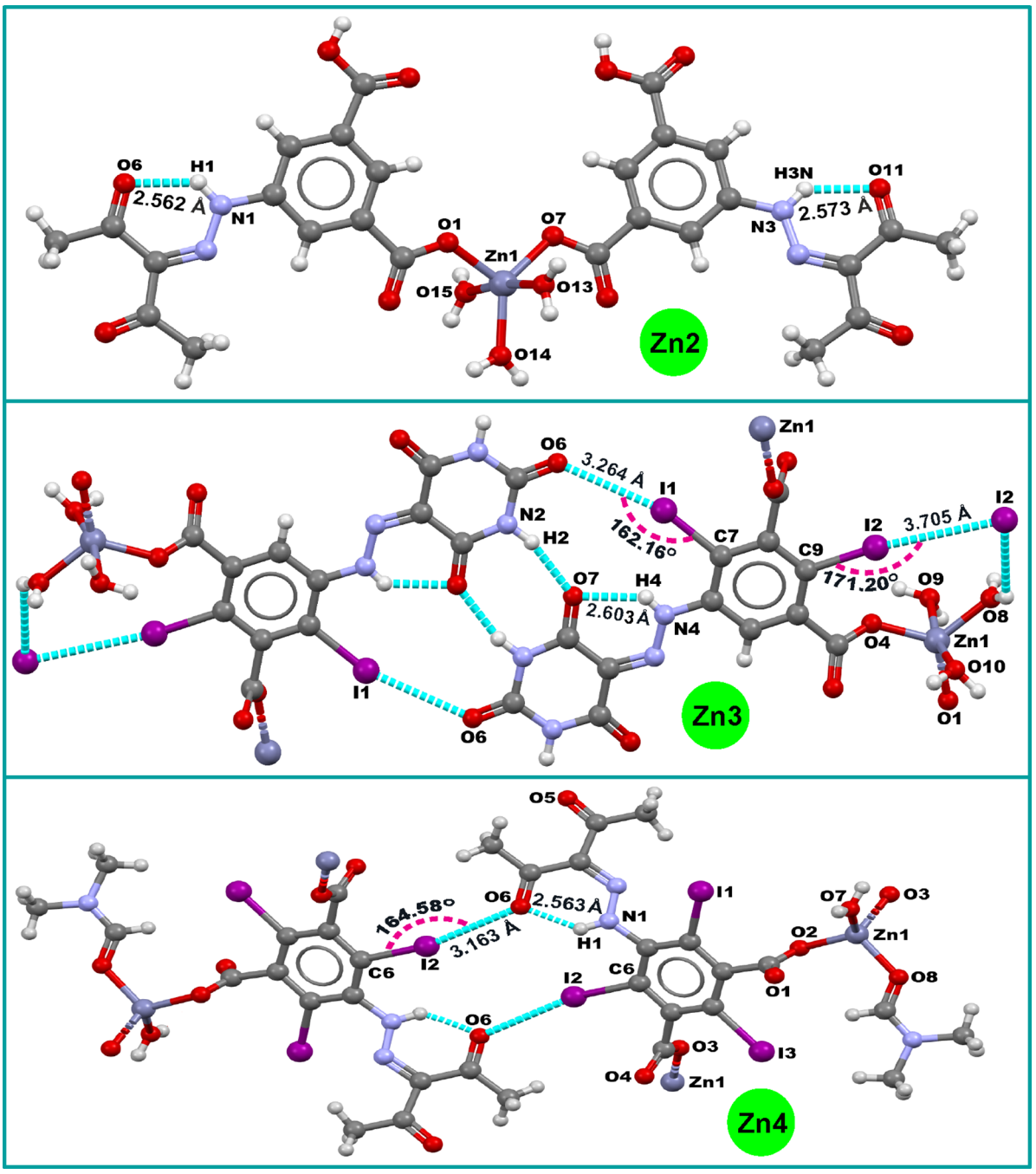

Figure 2. Molecular structures of **Zn2**, **Zn3**, and **Zn4**.

atoms, and the sum of the trigonal angles is 360°. The axial positions are occupied by the oxygen atoms of two water molecules, in which dihedral ∠O8−Zn1···O10 and ∠O8−Zn1···O9 angles are 81.88 and 84.73°, respectively. The crystal structure showed strong RAHB interactions between N(4)−H(4)···O(7) at distance of 2.603(6) Å. The intermolecular O(10)−H(10A)···O(3) (2.698 Å) hydrogen bond-assisted combination of two **Zn3** molecules leads to a zero-dimensional $R_2^2(12)$ aggregate[60] (Figure S2). Moreover, **Zn3** forms a zigzag chain 1D supramolecular polymer exclusively through N(1)−H(1)···O(6) (2.865 Å) and N(2)−H(2)···O(7) (2.870 Å) hydrogen bonds (Figure S3). In the packing structure of **Zn3**, there are ∠C(7)−I(1)···O(6) (162.16°) and ∠C(9)−I(2)···I(2) (171.20°) types of intermolecular halogen bonds with distances of 3.264 and 3.705 Å, respectively, both being significantly shorter than the sum of the Bondi's van der Waals radii of the interacting atoms (I + O = 1.98 + 1.52 = 3.50 Å and I + I = 1.98 + 1.98= 3.96 Å)[62] (Figure 2). Thus, a cooperation of these halogen bonds between tectons leads to 1D supramolecular polymer (Figure S4).

In **Zn4**, the Zn(II) center has a distorted tetrahedral geometry, with two oxygen donor atoms from the arylhydrazone ligands occupying two coordination sites along with one DMF and one water molecules occupying the other two sites (Figure 2). The tetrahedral environment around zinc is confirmed by the ∠O(2)−Zn(1)−O(7) (116.57°) and ∠O(2)−Zn(1)−O(8) (112.87°) angles with τ_4 index of 0.92.[63] The Zn−O bond lengths range from 1.914(4) to

https://doi.org/10.1021/acsomega.3c04262
ACS Omega 2023, 8, 42290−42300

1.985(5) Å. Similarly to **Zn2** and **Zn3**, the RAHB system [N···O distances of 2.563(8) Å] of **Zn4** does not participate in the coordination, but its carbonyl oxygen acts as the hydrogen and halogen bond acceptor (Figure 2). The intermolecular halogen bond assisted aggregation was found in the molecular packing of **Zn4**, in which the I(2)···O(6) (3.163 Å) distance is significantly shorter than the sum of van der Waals radii of the interacting atoms (Σr_{vdW} (I···O) = 3.50 Å (Figure 2). In addition, the ∠C(6)−I(2)···O(6) (164.58°) angle is consistent with the directionality term of halogen bonding.[64] The overall crystal structure is organized by strong hydrogen bonding interactions between the coordinated water hydrogens and both carboxylate and carbonyl groups in adjacent units (Figure S5).

3.2. Catalytic Activity of Zn(II)- and Cd(II)-Arylhydrazonates in the Cycloaddition Reaction of CO_2 with Epoxides. All Zn(II)- and Cd(II)-arylhydrazonate complexes, as well as $Zn(NO_3)_2{\cdot}4H_2O$, $Cd(NO_3)_2{\cdot}4H_2O$, $Zn(CH_3COO)_2{\cdot}2H_2O$, and $Cd(CH_3COO)_2{\cdot}2H_2O$, have been tested as homogeneous catalysts for the coupling of CO_2 with 2-phenyloxirane (as a model substrate) to produce the cyclic carbonate 4-phenyl-1,3-dioxolan-2-one under solvent-free conditions (Scheme 3, Table 2). As can be seen in Table 2 (entry 1), there is no reaction between the substrate and carbon dioxide in the absence of the cocatalyst, metal salts, or catalysts, while tetrabutylammonium bromide (TBABr) leads to the 15% yield of cyclic carbonate (entry 2). No cycloaddition reaction between CO_2 with 2-phenyloxirane takes place in the absence of the cocatalyst (TBABr), even in the presence of Zn(II)- and Cd(II)-salts or their arylhydrazonate complexes. $Zn(CH_3COO)_2{\cdot}2H_2O$, in the presence of TBABr, is slightly more active than the other salts (entries 3−6). As expected, due to high Lewis acidity, the Zn(II) complexes (mainly **Zn4**) are significantly more active in comparison to Cd(II)-arylhydrazonate (entries 7−16). Not only a change of the metal but also a modification of the active methylene fragment (compare acetylacetone with barbituric acid) in the arylhydrazone ligands, as well the use of halogen bond donor centers at their aromatic moiety, allows the yield of 4-phenyl-1,3-dioxolan-2-one to be increased (see Scheme 2 and entries 7−16). The iodo-substituted zinc compounds (**Zn3** and **Zn4**) are more active than the unsubstituted ones (compare entries 9 and 10 with entries 7, 8, and 11), and the same trend, although less pronounced, seems to occur within the less active cadmium series. Taking into consideration that the halogen bonded **Zn4** presented the highest catalytic activity, it was selected for further optimization.

Due to involvement in the ring-opening or ring-closure stage, the ionic cocatalysts tetrabutyl-ammonium chloride (TBACl), tetrabutylammonium bromide (TBABr), or tetrabutylammonium iodide (TBAI) have been widely used in the cycloaddition of CO_2 with epoxides.[65−69] Herein, we have studied the effect of TBACl, TBABr, TBAI, and tetrabutylammonium tetrafluoroborate ($TBABF_4$) on the **Zn4**-catalyzed coupling of CO_2 with 2-phenyloxirane, and the results (Table 3, entries 1−4) show the crucial role of anions in this reaction. Due to the expected participation of BF_4^- and Cl^- anions in strong intermolecular charge assisted hydrogen bonding,[65] both $TBABF_4$ and TBACl are not effective in the reaction, in contrast to weaker hydrogen bond acceptor and good leaving ability of Br^- and I^- in TBABr and TBAI, which can facilitate the ring-opening or ring-closure stage in the formation of cyclic

Scheme 3. Cycloaddition of CO_2 with 2-Phenyloxirane into 4-Phenyl-1,3-dioxolan-2-one

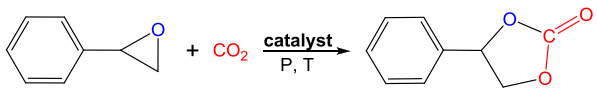

Table 2. Screening of Zn(II)- and Cd(II)-Arylhydrazonate Catalysts for the Reaction of CO_2 with 2-Phenyloxirane[a]

entry	catalyst	yield, %[b]
1	blank	
2	TBABr (cocatalyst)	15
3	$Zn(NO_3)_2{\cdot}4H_2O$	15
4	$Cd(NO_3)_2{\cdot}4H_2O$	11
5	$Zn(CH_3COO)_2{\cdot}2H_2O$	27
6	$Cd(CH_3COO)_2{\cdot}2H_2O$	17
7	**Zn1**	29
8	**Zn2**	49
9	**Zn3**	52
10	**Zn4**	56
11	**Zn5**	30
12	**Cd1**	17
13	**Cd2**	22
14	**Cd3**	23
15	**Cd4**	26
16	**Cd5**	19

[a]Catalyst 0.10 mol %, TBABr 0.4 mol %, T = 60 °C, P = 40 bar, 24 h. [b]Determined by ^{1}H NMR analysis (see Experimental Section).

Table 3. Effect of Cocatalyst, Reaction Time, Amount of Catalyst, Temperature, and Pressure on Zn4-Catalyzed Cycloaddition of CO_2 with 2-Phenyloxirane

entry	time, h	amount of catalyst, mol %	cocatalyst[a]	P, bar	T, °C	yield, %[b]
1	24	0.10	$TBABF_4$	40	60	0
2	24	0.10	TBACl	40	60	27
3	24	0.10	TBABr	40	60	56
4	24	0.10	TBAI	40	60	55
5	3	0.10	TBABr	40	60	9
6	6	0.10	TBABr	40	60	19
7	18	0.10	TBABr	40	60	39
8	24	0.10	TBABr	40	60	56
9	36	0.10	TBABr	40	60	62
10	48	0.10	TBABr	40	60	65
11	48	0.05	TBABr	40	60	48
12	48	0.10	TBABr	40	60	65
13	48	0.15	TBABr	40	60	66
14	48	0.20	TBABr	40	60	68
15	48	0.25	TBABr	40	60	70
16	48	0.30	TBABr	40	60	70
17	48	0.25	TBABr	10	60	57
18	48	0.25	TBABr	25	60	62
19	48	0.25	TBABr	40	60	70
20	48	0.25	TBABr	60	60	71
21	48	0.25	TBABr	40	20	1
22	48	0.25	TBABr	40	40	11
23	48	0.25	TBABr	40	60	70
24	48	0.25	TBABr	40	80	94

[a]0.4 mol % of cocatalyst. [b]Determined by ^{1}H NMR analysis (see Experimental Section).

https://doi.org/10.1021/acsomega.3c04262
ACS Omega 2023, 8, 42290−42300

carbonate.[65,68] Since TBABr appears to be an appropriate cocatalyst, it was used in further optimization experiments in this study.

As can been seen in Table 3 (entries 5−10), the yield of cyclic carbonate grows by increasing the reaction time, but after 36 h, it did not change considerably. After 48 h the yield of 4-phenyl-1,3-dioxolan-2-one reached 65% (entry 10), and this reaction time was maintained in the next steps. Next, the amount of catalyst in the conversion of 2-phenyloxirane was investigated (Table 3, entries 11−16). The increase of the catalyst amount up to 0.10 mol % loading resulted in a marked yield improvement of cyclic carbonate (entries 11 and 12), whereas a higher catalyst amount (0.10−0.25 mol %) had a much lower effect (entries 13−15), and a further increase to 0.30 mol % (entry 16) did not improve the product yield. Hence, the catalyst amount of 0.25 mol % was used as the optimal in the next steps. The catalytic activity of **Zn4** moderately decreased from 70 to 57% by reducing the initial CO_2 pressure from 40 and 10 bar (entries 19 to 17). The increase of CO_2 pressure from 40 to 60 bar does not affect the yield of 4-phenyl-1,3-dioxolan-2-one (entries 19 and 20), and thus further reactions were performed under 40 bar. The temperature (in the 20−80 °C range) also had a crucial promoting effect on the yield of the cyclic carbonate (entries 21−24), and a remarkable conversion (94%) of 2-phenyloxirane is observed at 80 °C.

Having the reaction conditions optimized (0.25 mol % of catalyst, 48 h, 40 bar, 80 °C), we investigated the reactivity of a variety of epoxides, and the appropriate cyclic carbonates were generally obtained in good yields (85−99%, Table 4).

Table 4. Cycloaddition Reaction of Various Epoxides and CO_2 Catalyzed by Zn4[a]

Entry	Substrate	Yield, %[b]
1	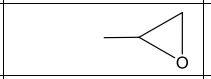	97
2	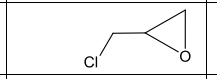	99
3	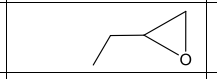	93
4	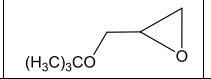	95
5	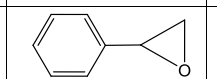	94
6	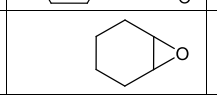	85

[a]Reaction conditions: epoxide (8.74 mmol), 0.25 mol % of catalyst, 0.40 mol % of cocatalyst, 48 h, 40 bar, 80 °C. [b]Determined by ^{1}H NMR analysis (see Experimental Section)

Epichlorohydrine bearing an electron-withdrawing chloro group exhibits the highest reactivity as compared to the electron-donating $-CH_3$, $-C_2H_5$ or $-OC(CH_3)_3$ group containing substrates (entries 1−4). In contrast to 2-phenyloxirane (entry 5) and other aliphatic epoxides (entries 1−4), 7-oxabicyclo[4.1.0]heptane showed a lower reactivity because of the rigidness of the chair conformation (entry 6).

The yields of 4-methyl-1,3-dioxolan-2-one (97%, entry 1) and 4-ethyl-1,3-dioxolan-2-one (93%, entry 3) observed in this work are higher than those reported[70] for a pyrrole-Schiff base zinc complex (74 and 81%, respectively) in the presence of cocatalyst TBABr, in which the use of dichloromethane as a solvent can also be considered a disadvantage in comparison to our solvent-free system. Relatively to **Zn4** (94%, entry 5, Table 4), the conversion of 2-phenyloxirane is also lower in the Zn(II)-*N,N-bis*(2-pyridinecarboxamide)-1,2-benzene/TBABr (27%),[71] Zn(II)-*bis*-thiosemicarbazonate/TBAI (29%),[72] Zn-(II)-*bis*(arylimino) acenaphthene)/TBABr (70%),[24] zinc(II)-azatrane/TBAI (75%),[73] and Zn(II)-[2-(4,5-diphenyl-1*H*-imidazol-2-yl)-4-((triphenylphosphonio)methyl)phenolate chloride]$_2$ (86%)[74] catalyzed systems.

Inspired on the reported[24,75−80] transition metal complex catalyzed reaction mechanism for cycloaddition of CO_2 with epoxides, we propose that the reaction proceeds as shown in Scheme 4, according to the following main steps with

Scheme 4. Proposed Reaction Mechanism of CO_2 Coupling with Epoxide, with Postulated Promoting Non-Covalent Interactions

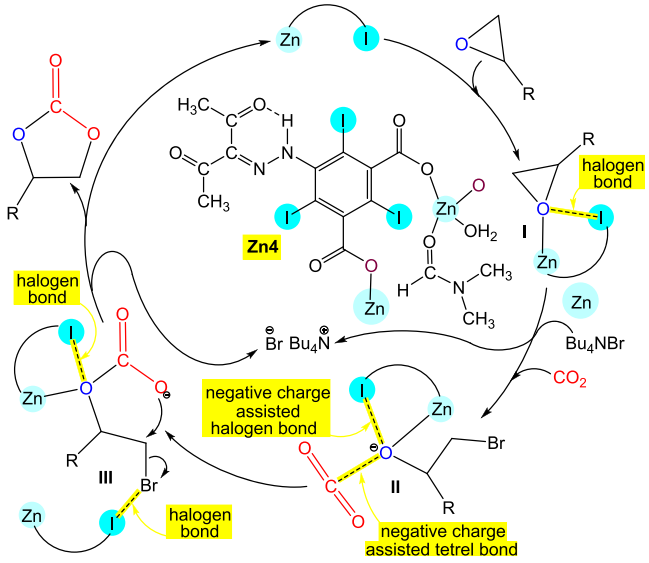

postulated involvement of iodo bonding: (i) ring opening in epoxide though its coordination to a metal center and conceivable halogen bonding with an iodo-substituent (**I**) and nucleophilic attack by halide anion; (ii) insertion of CO_2 possibly through the negative charge assisted halogen and tetrel bonding (**II**);[81] (iii) ring-closing (**III**) with liberation of cyclic carbonate and regeneration of the catalyst as well as of the halide anion (conceivably assisted by halogen bonding with a second catalyst molecule). Although the electron-withdrawing ability of the iodo-substitents in the ligand phenyl ring may increase the Lewis acidity of the metal center and thus promote the activation of the epoxide, we believe that this effect is much lower than that of the proposed iodo-bonding in view of the long distance of the iodo-substituents to the metal ion center (5 or 7 nonconjugated bonds), in contrast with the proposed iodo-bonding directly involving the epoxide.

4. CONCLUSIONS

Three new Zn(II)-arylhydrazonate complexes (**Zn2**, **Zn3**, and **Zn4**) were synthesized and structurally characterized. The

https://doi.org/10.1021/acsomega.3c04262
ACS Omega 2023, 8, 42290−42300

coordination environment around the zinc center and the supramolecular arrangement in these complexes are strongly dependent on the active methylene fragment (acetylacetone or barbituric acid) or the attached iodo-substituents at the aromatic moiety of the molecule. Not only normal intermolecular and strong intramolecular resonance assisted hydrogen bonds are present but there are also I···O and I···I types of halogen bonds in crystal packing of **Zn4** or **Zn3** leading to aggregates of 1D chains or 1D supramolecular chains, respectively.

In contrast to the metal−organic frameworks bearing derivatives of 5-aminoisophthalic acid in heterogeneous catalysts,[82,83] these new iodine-substituted complexes of arylhydrazones of isophthalic acid (**Zn3** and **Zn4**) are completely soluble in the substrates and act as homogenouse catalysts in added-solvent-free coupling of CO_2 with epoxides. According to our experiments, the following facts should be emphasized: (i) due to a higher Lewis acidity of the Zn center at **Zn3** and **Zn4**, these compounds show a higher catalytic activity in comparison to their Cd analogs (**Cd3** and **Cd4**) (see Table 2); (ii) the high solubility in epoxides (through intermolecular interactions, including halogen bonding) of the iodo-substituted compounds favors their catalytic activity in comparison with that of the unsubstituted ones (compare **Zn3** and **Zn4** with **Zn1**, **Zn2**, and **Zn5**, as well as **Cd3** and **Cd4** with **Cd1**, **Cd2**, and **Cd5** in Table 2); (iii) the active methylene fragment also affects the catalytic activity of the corresponding complexes (compare **Zn3** with **Zn4**, as well as **Cd3** with **Cd4** in Table 2); (iv) in the absence of cocatalyst (tetrabutylammonium bromide (TBABr)) all tested Cd and Zn complexes do not show catalytic activity; (v) **Zn4** is the most efficient catalyst for the cycloaddtion of CO_2 with both functionalized and nonfunctionalized epoxides in the presence of TBABr to produce the corresponding cyclic carbonates in high yields (85−99% after 48 h at 40 bar and 80 °C) (Table 4); (vi) the higher catalytic activity of the iodo-substituted complexes can be accounted for by considering the postulated promoting effect of halogen-bonding on the epoxide ring opening and on the ring closure step with CO_2 upon bromide extrusion.

In addition, it should be noted that this is the first report on the application of halogen bonded metal complexes in CO_2 coupling with epoxides, a topic which deserves to be further explored for other substrates such as diamines, diols, amino-diols, etc.

■ ASSOCIATED CONTENT

Supporting Information

The Supporting Information is available free of charge at https://pubs.acs.org/doi/10.1021/acsomega.3c04262.

Intermolecular noncovalent interactions in **Zn2**, **Zn3**, and **Zn4** in Figures S1−S5 (PDF)
(CIF)
(CIF)
(CIF)

■ AUTHOR INFORMATION

Corresponding Authors

Ana V. M. Nunes − *LAQV-REQUIMTE, Departamento de Química, Faculdade de Ciências e Tecnologia, Universidade Nova de Lisboa, Caparica 2829-516, Portugal*;
Email: ana.nunes@fct.unl.pt

Kamran T. Mahmudov − *Centro de Química Estrutural, Institute of Molecular Sciences, Instituto Superior Técnico, Universidade de Lisboa, Lisboa 1049-001, Portugal; Excellence Center, Baku State University, Baku 1148, Azerbaijan*; orcid.org/0000-0003-0743-6520;
Email: mahmudov.kt@gmail.com

Armando J. L. Pombeiro − *Centro de Química Estrutural, Institute of Molecular Sciences, Instituto Superior Técnico, Universidade de Lisboa, Lisboa 1049-001, Portugal*;
Email: pombeiro@tecnico.ulisboa.pt

Authors

Vusala A. Aliyeva − *Centro de Química Estrutural, Institute of Molecular Sciences, Instituto Superior Técnico, Universidade de Lisboa, Lisboa 1049-001, Portugal*

Ana B. Paninho − *LAQV-REQUIMTE, Departamento de Química, Faculdade de Ciências e Tecnologia, Universidade Nova de Lisboa, Caparica 2829-516, Portugal*

Anirban Karmakar − *Centro de Química Estrutural, Institute of Molecular Sciences, Instituto Superior Técnico, Universidade de Lisboa, Lisboa 1049-001, Portugal*; orcid.org/0000-0003-3047-2204

Atash V. Gurbanov − *Centro de Química Estrutural, Institute of Molecular Sciences, Instituto Superior Técnico, Universidade de Lisboa, Lisboa 1049-001, Portugal; Excellence Center, Baku State University, Baku 1148, Azerbaijan*

Arianna R. Rutigliano − *Centro de Química Estrutural, Institute of Molecular Sciences, Instituto Superior Técnico, Universidade de Lisboa, Lisboa 1049-001, Portugal; Department of Chemistry, University of Milan, Milan I-20133, Italy*

Emma Gallo − *Department of Chemistry, University of Milan, Milan I-20133, Italy*; orcid.org/0000-0002-2905-434X

Complete contact information is available at: https://pubs.acs.org/10.1021/acsomega.3c04262

Notes

The authors declare no competing financial interest.

■ ACKNOWLEDGMENTS

This work has been supported by the Fundação para a Ciência e a Tecnologia (FCT) (Portugal), projects UIDB/00100/2020, UIDP/00100/2020 and LA/P/0056/2020 of Centro de Química Estrutural, projects UIDB/50006/2020, UIDP/50006/2020 and LA/P/0008/2020 of the Associate Laboratory for Green Chemistry − LAQV REQUIMTE, and project MIT-EXPL/CS/0052/2021. A.V.G. and K.T.M. thank FCT and Instituto Superior Técnico (DL 57/2016, L 57/2017 and CEEC Institutional 2018 Programs, Contracts no: IST-ID/110/2018 and IST-ID/85/2018). VAA is grateful to Associação do Instituto Superior Técnico para Investigação e Desenvolvimento for her research fellowship through grant no: BL110/2022-IST-ID. K.T.M. and A.V.G. acknowledge the support by the Baku State University (Azerbaijan). A.R.R. thanks the Erasmus Program of the University of Milan and the Instituto Superior Técnico for a traineeship at the IST. Authors thank the Portuguese NMR Network (IST-UL Centre) and the IST Node of the Portuguese Network of mass-spectrometry. NMR spectrometers are part of The National NMR Facility, supported by FCT (ROTEIRO/0031/2013-PINFRA/22161/2016) (co- financed by FEDER

https://doi.org/10.1021/acsomega.3c04262
ACS Omega 2023, 8, 42290−42300

through COMPETE 2020, POCI, and PORL and FCT through PIDDAC).

REFERENCES

(1) Ding, M.; Flaig, R. W.; Jiang, H.-L.; Yaghi, O. M. Carbon capture and conversion using metal−organic frameworks and MOF-based materials. *Chem. Soc. Rev.* **2019**, *48*, 2783−2828.
(2) Bai, S. T.; Smet, G. D.; Liao, Y.; Sun, R.; Zhou, C.; Beller, M.; Maes, B. U. W.; Sels, B. F. Homogeneous and heterogeneous catalysts for hydrogenation of CO_2 to methanol under mild conditions. *Chem. Soc. Rev.* **2021**, *50*, 4259−4298.
(3) Ayyappan, R.; Abdalghani, I.; Da Costa, R. C.; Owen, G. R. Recent developments on the transformation of CO_2 utilising ligand cooperation and related strategies. *Dalton Trans.* **2022**, *51*, 11582−11611.
(4) *Climate Change: How Do We Know?*; 2020 https://climate.nasa.gov/evidence/, (accessed 16/06/2020).
(5) Guo, L.; Lamb, K. J.; North, M. Recent developments in organocatalysed transformations of epoxides and carbon dioxide into cyclic carbonates. *Green Chem.* **2021**, *23*, 77−118.
(6) Li, W.; Wang, H.; Jiang, X.; Zhu, J.; Liu, Z.; Guo, X.; Song, C. A short review of recent advances in CO_2 hydrogenation to hydrocarbons over heterogeneous catalysts. *RSC Adv.* **2018**, *8*, 7651−7669.
(7) Perathoner, S.; Van Geem, K. M.; Marin, G. B.; Centi, G. Reuse of CO2 in energy intensive process industries. *Chem. Commun.* **2021**, *57*, 10967−10982.
(8) Kamphuis, A. J.; Picchioni, F.; Pescarmona, P. P. CO2-fixation into cyclic and polymeric carbonates: principles and applications. *Green Chem.* **2019**, *21*, 406−448.
(9) Lopes, E. J. C.; Ribeiro, A. P. C.; Martins, L. M. D. R. S. New Trends in the Conversion of CO2 to Cyclic Carbonates. *Catalysts* **2020**, *10*, 479.
(10) Fernandes, D. M.; Peixoto, A. F.; Freire, C. Nitrogen-doped metal-free carbon catalysts for (electro)chemical CO_2 conversion and valorisation. *Dalton Trans.* **2019**, *48*, 13508−13528.
(11) Guo, F.; Zhang, X. Metal−organic frameworks for the energy-related conversion of CO2 into cyclic carbonates. *Dalton Trans.* **2020**, *49*, 9935−9947.
(12) Otto, A.; Grube, T.; Schiebahn, S.; Stolten, D. Closing the loop: captured CO_2 as a feedstock in the chemical industry. *Energy Environ. Sci.* **2015**, *8*, 3283−3297.
(13) Xu, J. H.; Peng, S. F.; Shi, Y. K.; Ding, S.; Yang, G. S.; Yang, Y. Q.; Xu, Y. H.; Jiang, C. J.; Su, Z. M. A novel zirconium-based metal−organic framework covalently modified by methyl pyridinium bromide for mild and co-catalyst free conversion of CO_2 to cyclic carbonates. *Dalton Trans.* **2023**, *52*, 659−667.
(14) Liu, Q.; Wu, L.; Jackstell, R.; Beller, M. Using carbon dioxide as a building block in organic synthesis. *Nat. Commun.* **2015**, *6*, 5933.
(15) Maeda, C.; Miyazaki, Y.; Ema, T. Recent progress in catalytic conversions of carbon dioxide. *Catal. Sci. Technol.* **2014**, *4*, 1482−1497.
(16) Fiorani, G.; Guo, W.; Kleij, A. W. Sustainable conversion of carbon dioxide: the advent of organocatalysis. *Green Chem.* **2015**, *17*, 1375−1389.
(17) Martín, C.; Fiorani, G.; Kleij, A. W. Recent Advances in the Catalytic Preparation of Cyclic Organic Carbonates. *ACS Catal.* **2015**, *5*, 1353−1370.
(18) Lan, D.-H.; Fan, N.; Wang, Y.; Gao, X.; Zhang, P.; Chen, L.; Au, C.-T.; Yin, S.-F. Recent advances in metal-free catalysts for the synthesis of cyclic carbonates from CO2 and epoxides. *Chin. J. Catal.* **2016**, *37*, 826−845.
(19) Comerford, J. W.; Ingram, I. D. V.; North, M.; Wu, X. Sustainable metal-based catalysts for the synthesis of cyclic carbonates containing five-membered rings. *Green Chem.* **2015**, *17*, 1966−1987.
(20) He, Q.; O'Brien, J. W.; Kitselman, K. A.; Tompkins, L. E.; Curtis, G. C. T.; Kerton, F. M. Synthesis of cyclic carbonates from CO2 and epoxides using ionic liquids and related catalysts including choline chloride−metal halide mixtures. *Catal. Sci. Technol.* **2014**, *4*, 1513−1528.
(21) Cokoja, M.; Wilhelm, M. E.; Anthofer, M. H.; Herrmann, W. A.; Kühn, F. E. Synthesis of Cyclic Carbonates from Epoxides and Carbon Dioxide by Using Organocatalysts. *ChemSusChem* **2015**, *8*, 2436−2454.
(22) Shaikh, R. R.; Pornpraprom, S.; D'Elia, V. Catalytic Strategies for the Cycloaddition of Pure, Diluted, and Waste CO2 to Epoxides under Ambient Conditions. *ACS Catal.* **2018**, *8*, 419−450.
(23) Montoya, C. A.; Gómez, C. F.; Paninho, A. B.; Nunes, A. V. M.; Mahmudov, K. T.; Najdanovic-Visak, V.; Martins, L. M. D. R. S.; Guedes Da Silva, M. F. C.; Pombeiro, A. J. L.; Nunes Da Ponte, M. Cyclic carbonate synthesis from CO_2 and epoxides using zinc(II) complexes of arylhydrazones of β-diketones. *J. Catal.* **2016**, *335*, 135−140.
(24) Zakrzewska, M. E.; André, P. J. L.; Gomes, C. S. B.; Nunes, A. V. M.; Rosa, V. Zinc complexes bearing BIAN ligands as efficient catalysts for the formation of cyclic carbonates from CO_2 and epoxides. *New J. Chem.* **2023**, *47*, 6551−6562.
(25) Paninho, A. B.; Ventura, A. L. R.; Branco, L. C.; Pombeiro, A. J. L.; da Silva, M. F. C. G. G.; da Ponte, M. N.; Mahmudov, K. T.; Nunes, A. V. M. CO_2 + ionic liquid biphasic system for reaction/product separation in the synthesis of cyclic carbonates. *J. Supercrit. Fluids* **2018**, *132*, 71−75.
(26) Li, Y.; Liu, S.; Zhao, X.; Wang, Y.; Liu, J.; Wang, X.; Lu, L. CO_2-based amphiphilic polycarbonate micelles enable a reliable and efficient platform for tumor imaging. *Theranostics* **2017**, *7*, 4689−4698.
(27) Liu, Y.; Huang, K.; Peng, D.; Liu, S.; Wu, H. Preparation of poly(butylene-co-ε -caprolactone carbonate) and their use as drug carriers for a controlled delivery system. *J. Polym. Sci., Part A: Polym. Chem.* **2007**, *45*, 2152−2160.
(28) Li, H.; Niu, Y. Preparation of poly(propylene carbonate-co-ε-caprolactone) and their applications in drug delivery. *Int. J. Polym. Mater. Polym. Biomater.* **2018**, *67*, 192−198.
(29) Xu, K. Nonaqueous Liquid Electrolytes for Lithium-Based Rechargeable Batteries. *Chem. Rev.* **2004**, *104*, 4303−4418.
(30) *Lithium-Ion Rechargeable Batteries*; Ed. Ozawa, K. Wiley-VCH Verlag GmbH & Co. KGaA: Tokyo, 2009.
(31) Marquis, E. T.; Baldwin, R. E.; Machac, J. R.; Darragas, K.; Woodrum, S. A. WO Pat, 2001042376A1, 2001.
(32) Parker, H. L.; Sherwood, J.; Hunt, A. J.; Clark, J. H. Cyclic Carbonates as Green Alternative Solvents for the Heck Reaction. *ACS Sustainable Chem. Eng.* **2014**, *2*, 1739−1742.
(33) Bello Forero, J. S.; Hernández Muñoz, J. A.; Jones Junior, J.; da Silva, F. M. Propylene Carbonate in Organic Synthesis: Exploring its Potential as a Green Solvent. *Curr. Org. Synth.* **2016**, *13*, 834−846.
(34) Guo, W.; Gómez, J. E.; Cristófol, Á.; Xie, J.; Kleij, A. W. Catalytic Transformations of Functionalized Cyclic Organic Carbonates. *Angew. Chem., Int. Ed.* **2018**, *57*, 13735−13747.
(35) Olsén, P.; Oschmann, M.; Johnston, E. V.; Akermark, B. Synthesis of highly functional carbamates through ring-opening of cyclic carbonates with unprotected α-amino acids in water. *Green Chem.* **2018**, *20*, 469−475.
(36) Mahmudov, K. T.; Gurbanov, A. V.; Guseinov, F. I.; Guedes da Silva, M. F. C. Noncovalent interactions in metal complex catalysis. *Coord. Chem. Rev.* **2019**, *387*, 32−46.
(37) *Noncovalent Interactions in Catalysis*; Mahmudov, K. T.; Kopylovich, M. N.; Guedes da Silva, M. F. C.; Pombeiro, A. J. L. (Eds.) Royal Society of Chemistry: UK, 2019.
(38) Bertani, R.; Sgarbossa, P.; Venzo, A.; Lelj, F.; Amati, M.; Resnati, G.; Pilati, T.; Metrangolo, P.; Terraneo, G. Halogen bonding in metal-organic-supramolecular networks. *Coord. Chem. Rev.* **2010**, *254*, 677−695.
(39) Mahmudov, K. T.; Gurbanov, A. V.; Aliyeva, V. A.; Guedes da Silva, M. F. C.; Resnati, G.; Pombeiro, A. J. L. Chalcogen bonding in coordination chemistry. *Coord. Chem. Rev.* **2022**, *464*, No. 214556.
(40) Mahmudov, K. T.; Gurbanov, A. V.; Aliyeva, V. A.; Resnati, G.; Pombeiro, A. J. L. Pnictogen bonding in coordination chemistry. *Coord. Chem. Rev.* **2020**, *418*, No. 213381.

https://doi.org/10.1021/acsomega.3c04262
ACS Omega 2023, 8, 42290−42300

(41) Gurbanov, A. V.; Kuznetsov, M. L.; Karmakar, A.; Aliyeva, V. A.; Mahmudov, K. T.; Pombeiro, A. J. L. Halogen bonding in cadmium(ii) MOFs: its influence on the structure and on the nitroaldol reaction in aqueous medium. *Dalton Trans.* **2022**, *51*, 1019−1031.
(42) Mahmudov, K. T.; Pombeiro, A. J. L. Control of Selectivity in Homogeneous Catalysis through Noncovalent Interactions. *Chem. - Eur. J.* **2023**, *29*, No. e202203861.
(43) Chen, K.; Yan, R.; Li, Z.; Huang, W.; Gao, L.; Duan, T.; Tong, H.; Li, Y.; Sun, J.; Guo, K. Halogen bonding catalysis for the [3 + 2] cycloaddition reactions of epoxides with CO2, and other hetero-cumulenes. *J. CO2 Util.* **2021**, *52*, No. 101663.
(44) Yan, R.; Chen, K.; Li, Z.; Qu, Y.; Gao, L.; Tong, H.; Li, Y.; Li, J.; Hu, Y.; Guo, K. Fixation of CO_2 into Cyclic Carbonates by Halogen-Bonding Catalysis. *ChemSusChem* **2021**, *14*, 738−744.
(45) Karmakar, A.; Paul, A.; Mahmudov, K. T.; Guedes da Silva, M. F. C.; Pombeiro, A. J. L. pH dependent synthesis of Zn(II) and Cd(II) coordination polymers with dicarboxyl-functionalized arylhydrazone of barbituric acid: photoluminescence properties and catalysts for Knoevenagel condensation. *New J. Chem.* **2016**, *40*, 1535−1546.
(46) Zamanloo, M. R.; Shamkhali, A.; Alizadeh, M.; Mansoori, Y.; Imanzadeh, G. A novel barbituric acid-based azo dye and its derived polyamides: Synthesis, spectroscopic investigation and computational calculations. *Dyes Pigm.* **2012**, *95*, 587−599.
(47) *SMART & SAINT Software Reference Manuals, Version 6.22*; Bruker AXS Analytic X-ray Systems, Inc.: Madison, WI, 2000.
(48) Sheldrick, G. M. *SADABS Software for Empirical Absorption Correction*; University of Göttingen: Germany, 2000.
(49) Sheldrick, G. M. *SHELXTL V5.1, Software Reference Manual*; Bruker AXS Inc.: Madison, WI, 1997.
(50) Sopeca, S.; Laserna, V.; Guo, W.; Martin, E.; Escudero-Adán, E. C. A. W. Kleij, Regioselective Organocatalytic Formation of Carbamates from Substituted Cyclic Carbonates. *Adv. Synth. Catal.* **2016**, *358*, 2172−2178.
(51) Steinbauer, J.; Spannenberg, A.; Werner, T. An in situ formed Ca^{2+}−crown ether complex and its use in CO_2-fixation reactions with terminal and internal epoxides. *Green Chem.* **2017**, *19*, 3769−3779.
(52) Li, C. Y.; Su, Y. C.; Lin, C. H.; Huang, H. Y.; Tsai, C. Y.; Lee, T. Y.; Ko, B. T. Synthesis and characterization of trimetallic cobalt, zinc and nickel complexes containing amine-bis(benzotriazole phenolate) ligands: efficient catalysts for coupling of carbon dioxide with epoxides. *Dalton Trans.* **2017**, *46*, 15399−15406.
(53) Wang, G.; Xu, C.; Wang, L.; Liu, W. Highly efficient 3d/4d−4f coordination polymer catalysts for carbon dioxide fixation into cyclic carbonates. *Dalton Trans.* **2018**, *47*, 12711−12717.
(54) Álvarez-Miguel, L.; Damián Burgoa, J.; Mosquera, M. E. G.; Hamilton, A.; Whiteoak, C. J. Catalytic Formation of Cyclic Carbonates using Gallium Aminotrisphenolate Compounds and Comparison to their Aluminium Congeners: A Combined Experimental and Computational Study. *ChemCatChem.* **2021**, *13*, 4099−4110.
(55) Tudu, G.; Paliwal, K. S.; Ghosh, S.; Biswas, T.; Koppisetti, H. V. S. R. M.; Mitra, A.; Mahalingam, V. para-Aminobenzoic acid-capped hematite as an efficient nanocatalyst for solvent-free CO2 fixation under atmospheric pressure. *Dalton Trans.* **2022**, *51*, 1918−1926.
(56) Saini, S.; Khan, S. R.; Gour, N. K.; Deka, R. C.; Jain, S. L. Metal-free, redox-neutral, and visible light-triggered coupling of CO2 with epoxides to cyclic carbonates at atmospheric pressure. *Green Chem.* **2022**, *24*, 3644−3650.
(57) Mahmudov, K. T.; Kopylovich, M. N.; Pombeiro, A. J. L. Coordination chemistry of arylhydrazones of methylene active compounds. *Coord. Chem. Rev.* **2013**, *257*, 1244−1281.
(58) Gurbanov, A. V.; Kuznetsov, M. L.; Demukhamedova, S. D.; Alieva, I. N.; Godjaev, N. M.; Zubkov, F. I.; Mahmudov, K. T.; Pombeiro, A. J. L. Role of substituents on resonance assisted hydrogen bonding vs. intermolecular hydrogen bonding. *CrystEngComm* **2020**, *22*, 628−633.
(59) Kopylovich, M. N.; Mahmudov, K. T.; Guedes da Silva, M. F. C.; Martins, L. M. D. R. S.; Kuznetsov, M. L.; Silva, T. F. S.; Fraústo da Silva, J. J. R.; Pombeiro, A. J. L. Trends in properties of para-substituted 3-(phenylhydrazo)pentane-2,4-diones. *J. Phys. Org. Chem.* **2011**, *24*, 764−773.
(60) Hughes, D. S.; Delori, A.; Rehman, A.; Jones, W. Using crystallography, topology and graph set analysis for the description of the hydrogen bond network of triamterene: a rational approach to solid form selection. *Chem. Central J.* **2017**, *11*, 63.
(61) Addison, A. W.; Rao, T. N.; Reedijk, J.; van Rijn, J.; Verschoor, G. C. Synthesis, structure, and spectroscopic properties of copper(II) compounds containing nitrogen−sulphur donor ligands; the crystal and molecular structure of aqua[1,7-bis(*N*-methylbenzimidazol-2′-yl)-2,6-dithiaheptane]copper(II) perchlorate. *J. Chem. Soc., Dalton Trans.* **1984**, 1349−1356.
(62) Bondi, A.; Van der. Waals Volumes and Radii. *J. Phys. Chem.* **1964**, *68*, 441−451.
(63) Yang, L.; Powell, D. R.; Houser, R. P. Structural variation in copper(i) complexes with pyridylmethylamide ligands: structural analysis with a new four-coordinate geometry index, τ_4. *Dalton Trans.* **2007**, 955−964.
(64) Cavallo, G.; Metrangolo, P.; Milani, R.; Pilati, T.; Priimagi, A.; Resnati, G.; Terraneo, G. The Halogen Bond. *Chem. Rev.* **2016**, *116*, 2478−2601.
(65) Liu, M.; Lan, J.; Liang, L.; Sun, J.; Arai, M. Heterogeneous catalytic conversion of CO_2 and epoxides to cyclic carbonates over multifunctional tri-s-triazine terminal-linked ionic liquids. *J. Catal.* **2017**, *347*, 138−147.
(66) Wang, L.; Zhang, G.; Kodama, K.; Hirose, T. An efficient metal- and solvent-free organocatalytic system for chemical fixation of CO_2 into cyclic carbonates under mild conditions. *Green Chem.* **2016**, *18*, 1229−1233.
(67) Alassmy, Y. A.; Pour, Z. A.; Pescarmona, P. P. Efficient and Easily Reusable Metal-Free Heterogeneous Catalyst Beads for the Conversion of CO_2 into Cyclic Carbonates in the Presence of Water as Hydrogen-Bond Donor. *ACS Sustainable Chem. Eng.* **2020**, *8*, 7993−8003.
(68) Zhang, Y. Y.; Yang, G. W.; Xie, R.; Yang, L.; Li, B.; Wu, G. P. Scalable, Durable, and Recyclable Metal-Free Catalysts for Highly Efficient Conversion of CO_2 to Cyclic Carbonates. *Angew. Chem., Int. Ed.* **2020**, *59*, 23291−23298.
(69) Cabrera, D. J.; Lewis, R. D.; Díez-Poza, C.; Álvarez-Miguel, L.; Mosquera, M. E. G.; Hamilton, A.; Whiteoak, C. J. Group 13 salphen compounds (In, Ga and Al): a comparison of their structural features and activities as catalysts for cyclic carbonate synthesis. *Dalton Trans.* **2023**, *52*, 5882−5894.
(70) de la Pena, M. A.; Merzoud, L.; Lamine, W.; Tuel, A.; Chermette, H.; Christ, L. Robust pyrrole-Schiff base Zinc complexes as novel catalysts for the selective cycloaddition of CO_2 to epoxides. *J. CO2 Util.* **2021**, *44*, No. 101380.
(71) Adolph, M.; Zevaco, T. A.; Altesleben, C.; Staudt, S.; Dinjus, E. New zinc catalysts based on easy-to-handle N4-chelating ligands for the coupling reaction of epoxides with CO_2. *J. Mol. Catal. A: Chem.* **2015**, *400*, 104−110.
(72) Anselmo, D.; Bocokić, V.; Decortes, A.; Escudero-Adán, E. C.; Benet-Buchholz, J.; Reek, J. N. H.; Kleij, A. W. Mild formation of cyclic carbonates using Zn(II) complexes based on N_2S_2-chelating ligands. *Polyhedron* **2012**, *32*, 49−53.
(73) Bousquet, B.; Martinez, A.; Dufaud, V. Zinc−Azatrane Complexes as Efficient Catalysts for the Conversion of Carbon Dioxide into Cyclic Carbonates. *ChemCatChem.* **2018**, *10*, 843−848.
(74) Peng, J.; Yang, H.-J.; Wang, S.; Ban, B.; Wei, Z.; Lei, B.; Guo, C. Y. Efficient solvent-free fixation of CO_2 catalyzed by new recyclable bifunctional metal complexes. *J. CO2 Util.* **2018**, *24*, 1−9.
(75) Castro-Gómez, F.; Salassa, G.; Kleij, A. W.; Bo, C. A DFT Study on the Mechanism of the Cycloaddition Reaction of CO_2 to Epoxides Catalyzed by Zn(Salphen) Complexes. *Chem. - Eur. J.* **2013**, *19*, 6289−6298.

https://doi.org/10.1021/acsomega.3c04262
ACS Omega 2023, 8, 42290−42300

(76) Zhang, F.; Wang, Y.; Zhang, X.; Zhang, X.; Liu, H.; Han, B. Recent advances in the coupling of CO2 and epoxides into cyclic carbonates under halogen-free condition. *Green Chem. Eng.* **2020**, *1*, 82−93.
(77) Kumar, M. D.; Sunny, S.; Jaccob, M. Conversion of CO_2 to cyclic carbonates by metal-ethylenediamine complexes in ionic liquid: A DFT mechanistic study. *J. CO2 Util.* **2022**, *57*, No. 101872.
(78) Yang, H.; Xie, Y.; Chen, W.; Tang, X.; Hu, M.; Shu, Y.; Wang, L.; Liu, W. Gridlike 3d-4f heterometallic macrocycles for highly efficient conversion of CO_2 into cyclic carbonates. *J. CO2 Util.* **2021**, *54*, No. 101780.
(79) Zhou, F.; Deng, Q.; Huang, N.; Zhou, W.; Deng, W. CO_2 Fixation into Cyclic Carbonates by a Zn-Salen Based Conjugated Microporous Polymer. *ChemistrySelect* **2020**, *5*, 10516−10520.
(80) Wu, T.; Wang, T.; Sun, L.; Deng, K.; Deng, W.; Lu, R. A DFT Exploration of Efficient Catalysts Based on Metal-Salen Monomers for the Cycloaddition Reaction of CO_2 to Propylene Oxide. *ChemistrySelect* **2017**, *2*, 4533−4537.
(81) Grabowski, S. J. Tetrel bond−σ-hole bond as a preliminary stage of the S_N2 reaction. *Phys. Chem. Chem. Phys.* **2014**, *16*, 1824−1834.
(82) Ning, L.; Liao, S.; Liu, X.; Yu, L.; Zhuang, X.; Tong, X. Selective transformation of renewable furfural catalyzed by diverse active species derived from 2D co-based metal-organic frameworks. *J. Catal.* **2017**, *352*, 480−490.
(83) Karmakar, A.; Pombeiro, A. J. L. Recent advances in amide functionalized metal organic frameworks for heterogeneous catalytic applications. *Coord. Chem. Rev.* **2019**, *395*, 86−129.

Recommended by ACS

Triiodide-Based Chair-Like Copper Complex Assembled by Halogen Bonding
Mikhail A. Kinzhalov, Nadezhda A. Bokach, *et al.*
DECEMBER 18, 2023
INORGANIC CHEMISTRY
READ

Exploring C–F···π Interactions: Synthesis, Characterization, and Surface Analysis of Copper β-Diketone Complexes
Babak Mirtamizdoust, Ajay Kumar Mishra, *et al.*
JANUARY 24, 2024
ACS OMEGA
READ

Preparation of Well-Defined Double-Metal Cyanide Catalysts for Propylene Oxide Polymerization and CO_2 Copolymerization
Yeong Hyun Seo, Bun Yeoul Lee, *et al.*
JANUARY 02, 2024
INORGANIC CHEMISTRY
READ

Theoretical Analysis of Cu^{II}···Cl Semicoordination Bond in Supramolecular Heterometallic $\{Cu^{II}\}\{Sn^{IV}\}$ Cocrystals
Susanta Hazra, Armando J. L. Pombeiro, *et al.*
SEPTEMBER 08, 2023
ORGANOMETALLICS
READ

Get More Suggestions >

https://doi.org/10.1021/acsomega.3c04262
ACS Omega 2023, 8, 42290−42300